Table 2. Mean value of $ICRU_{RP}$ or dose–volume parameters according to rectal bleeding

	Mean dose ± SD ($Gy_{\alpha\ \beta\ 3}$)			
Variable	Overall	Bleeding (-)	Bleeding (+)	p*
$ICUR_{RP}$	69 ± 17	64 ± 17	83 ± 20	<0.001
D_{2cc}	72 ± 16	68 ± 15	85 ± 14	<0.001
D_{1cc}	82 ± 2	76 ± 15	98 ± 19	<0.001
$D_{0.1cc}$	117 ± 49	107 ± 47	145 ± 41	0.004

Abbreviation: $ICRU_{RP}$ = International Commission on Radiation Units and Measurements Report 38 rectal reference point; D_{2cc}, D_{1cc}, $D_{0.1cc}$ = minimum dose received by the 2-cm^3, 1-cm^3, and 0.1-cm^3 volumes with the highest irradiation, respectively.
* Student's t test.

symptoms requiring no treatment; Grade 2 to symptoms responding to simple outpatients management; Grade 3 to distressing symptoms requiring hospitalization for diagnosis, minor intervention, or transfusion; and Grade 4 to fistula formation or the need for major surgical intervention.

Source strength

Data for the ^{192}Ir source strength were collected on each day of the HDR-ICBT session, and the average source strength was calculated over three or four ICBT sessions.

Statistical analysis

The actuarial rate of rectal bleeding was estimated using the Kaplan-Meier method, and differences between factors were examined with the log-rank test. Student's t-test was used to compare the mean dose when the rectal bleeding occurred to the mean dose without using the dose–volume parameters (D_{2cc}, D_{1cc}, $D_{0.1cc}$) or $ICRU_{RP}$ data.

RESULTS

Of the 62 patients, 17 (27%) developed late rectal bleeding, including 13 (21%) with Grade 1 toxicity, 2 (3%) with Grade 2, 0 (0%) with Grade 3, and 2 (3%) with Grade 4. The median EQD_2 representing the sum of the EBRT and HDR-ICRT dose was 65 Gy (range, 22-118 Gy) for $ICRU_{RP}$, 71 Gy (range, 29–112 Gy) for D_{2cc}, 80 Gy (range, 32–150 Gy) for D_{1cc}, and 108 Gy (range, 39–285 Gy) for $D_{0.1cc}$. Differences in the mean EQD_2 dose for patients with or without rectal bleeding are shown in Table 2. Patients with rectal bleeding received a significantly greater nominal total dose for $ICRU_{RP}$ ($p < 0.001$), D_{2cc} ($p < 0.001$), D_{1cc} ($p < 0.001$), and $D_{0.1cc}$ ($p = 0.004$). The patients were divided into low-EQD_2 (<median dose) and high-EQD_2 (≥median dose) groups. The actuarial rectal bleeding rate for each group is shown in Fig. 1. The 2-year rectal bleeding rates for the low-EQD_2 and high-EQD_2 groups were, respectively, 12% and 47% for $ICRU_{RP}$, 15% and 44% for D_{2cc}, 12% and 47% for D_{1cc}, and 8% and 51% for $D_{0.1cc}$. The high-EQD_2 group had a significantly greater rectal bleeding risk for all parameters ($ICRU_{RP}$, D_{2cc}, D_{1cc}, and $D_{0.1cc}$).

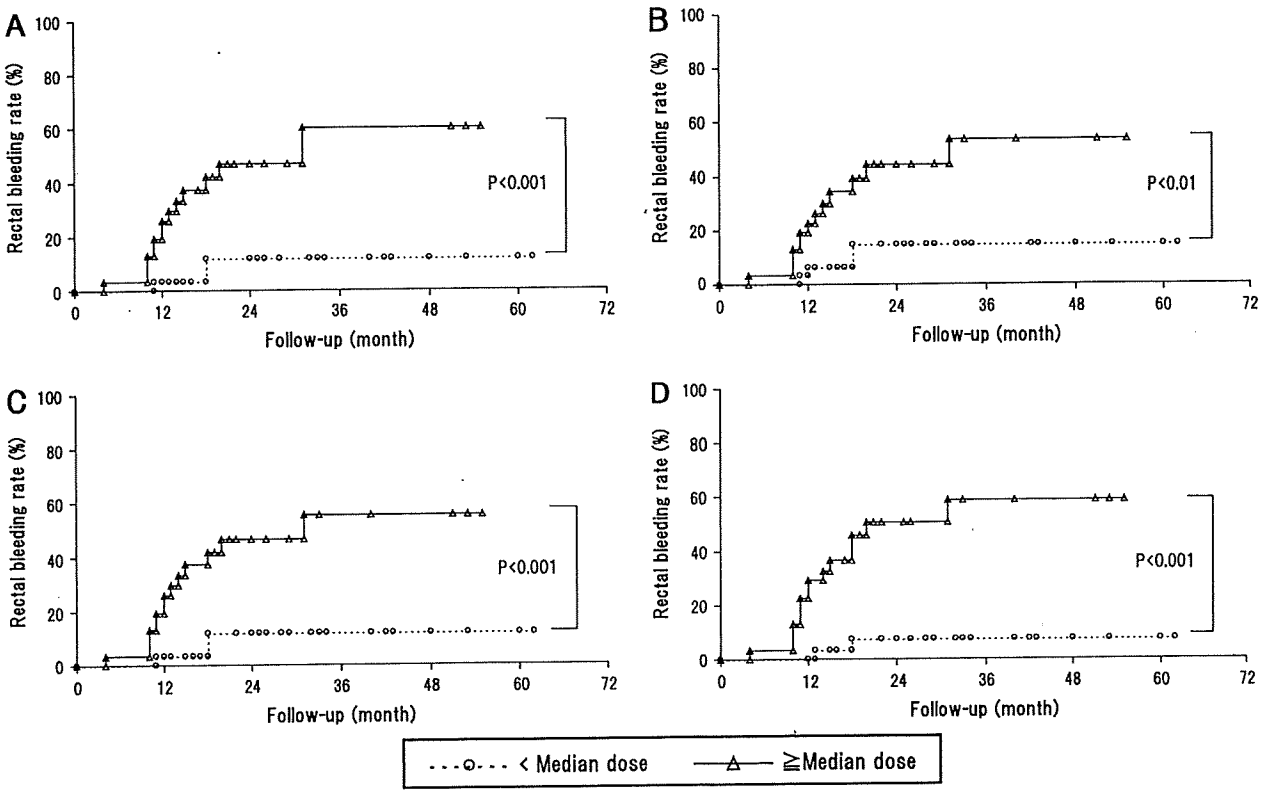

Fig. 1. Actuarial rectal bleeding rates for two groups based on the biologically equivalent dose in 2-Gy fractions (EQD_2) (<median dose vs. ≥median dose for each parameter). (A) International Commission on Radiation Units and Measurements Report 38 rectal reference point ($ICRU_{RP}$) (B) D_{2cc}. (C) D_{1cc}. (D) $D_{0.1cc}$.

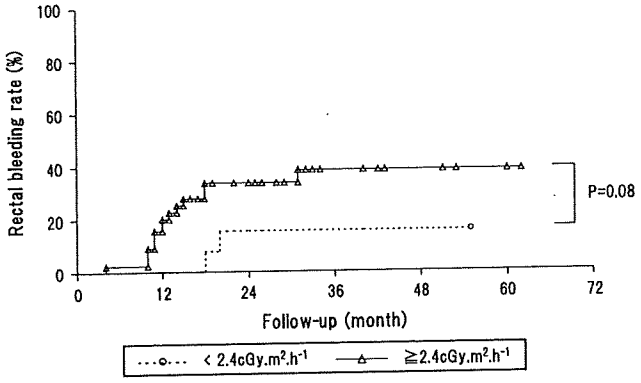

Fig. 2. Actuarial rectal bleeding rates for two groups based on ^{192}Ir source strength threshold values of 2.4 cGy.m^2.h^{-1}.

Patients were also divided into two groups based on the threshold source strength of 2.4 cGy.m^2.h^{-1} (the median source strength was 2.512 cGy.m^2.h^{-1} with a range of 1.904–4.631 cGy.m^2.h^{-1}). The group with the stronger source strength showed greater rectal bleeding, but the difference was not statistically significant (15% vs. 34% at 2 years; $p = 0.08$), as shown in Fig. 2.

Next, the patients were separated into four groups according to the median rectal EQD_2 and the threshold source strength of 2.4 cGy.m^2.h^{-1}; Group 1 (<median dose and <2.4 cGy.m^2.h^{-1}), Group 2 (<median dose and ≥2.4 cGy.m^2.h^{-1}), Group 3 (≥median dose and <2.4 cGy.m^2.h^{-1}), and Group 4 (≥median dose and ≥2.4 cGy.m^2.h^{-1}). The actuarial rectal bleeding rate for each group is shown in Fig. 3. There was a significant difference in rectal bleeding between Group 4 and Groups 1–3 for $ICRU_{RP}$, D_{2cc}, and D_{1cc}. For EQD_2 at $D_{0.1cc}$, there was a significant difference in rectal bleeding between Group 4 and Groups 1 and 2. Group 4 also had greater rectal bleeding than Group 3, but the difference was not statistically significant ($p = 0.1$). The relationship between the rectal dose and source strength for each patient is also shown in Fig. 4. Correlation coefficient analysis showed no significant relationship between rectal dose and source strength. Both patients with Grade 4 rectal bleeding were in Group 4. Clinical parameters of patients who did and did not develop late rectal bleeding were also compared (Table 3), but there was no significant difference between the two groups regarding age (<70 vs. ≥70 years old), stage (Stage I-II vs. Stage III-IV), or concurrent chemotherapy (No vs. Yes).

DISCUSSION

In a previous report, we demonstrated that patients with not only BED ≥100 Gy_3 but also an average source strength of >2.4 cGy.m^2.h^{-1} showed a correlation with a high incidence of rectal bleeding (5). To our knowledge, this was the first report to demonstrate the effect of source strength

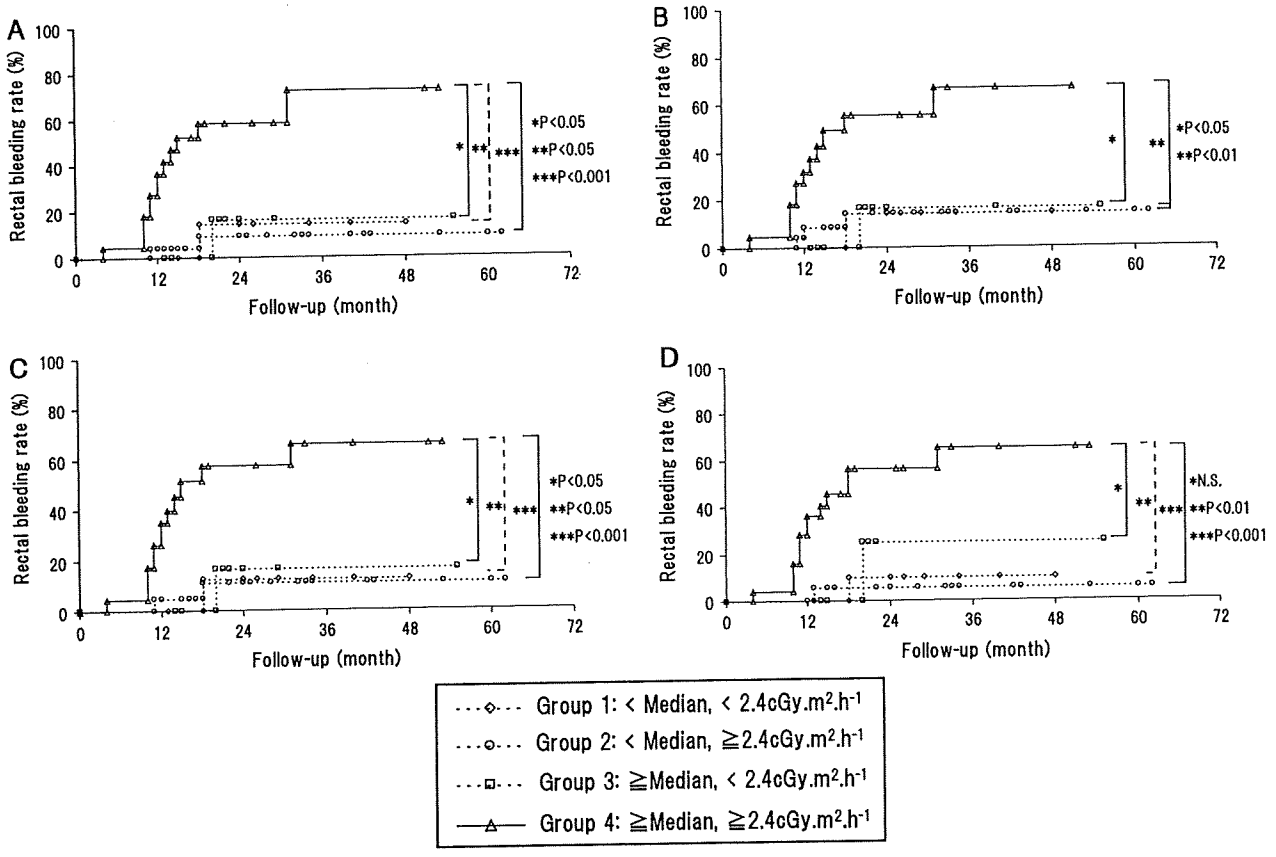

Fig. 3. Actuarial rectal bleeding rates for four groups based on the threshold values of the median dose and the source strength of 2.4 cGy.m^2.h^{-1}. (A) International Commission on Radiation Units and Measurements Report 38 rectal reference point ($ICRU_{RP}$). (B) D_{2cc}. (C) D_{1cc}. (D) $D_{0.1cc}$.

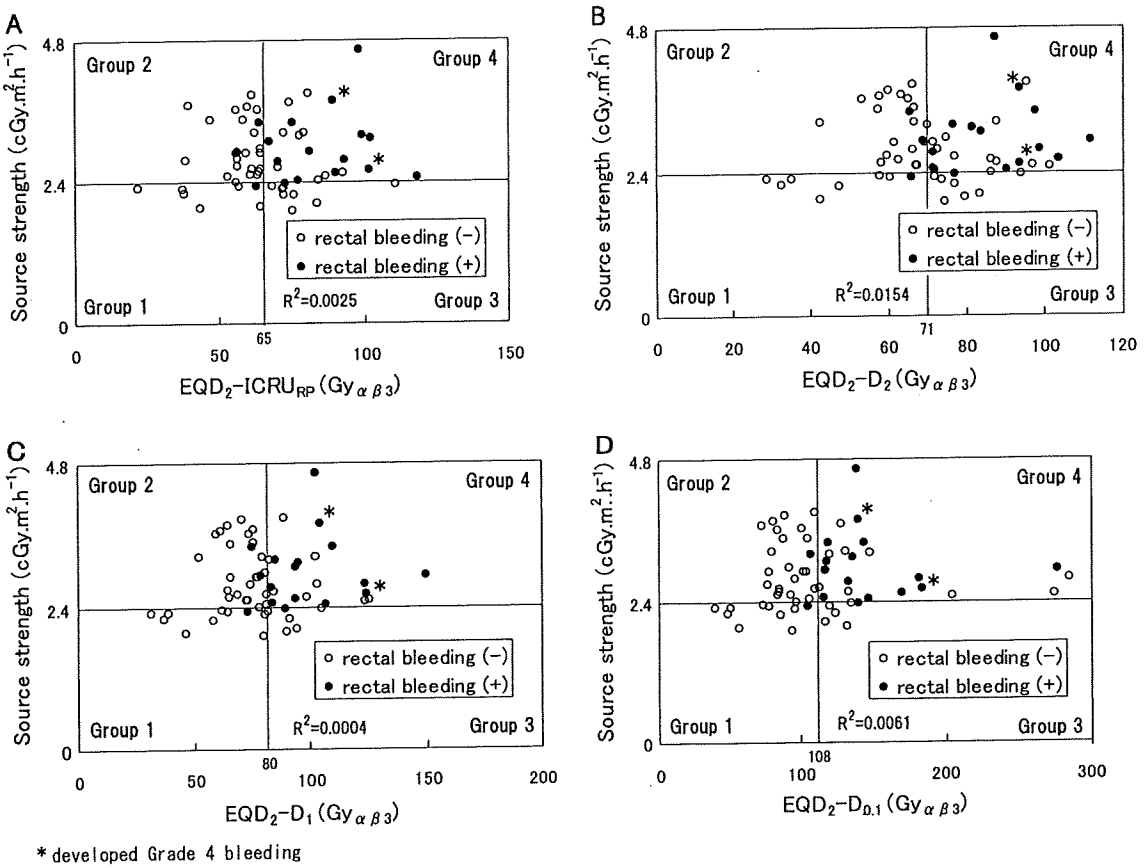

Fig. 4. Relationship of rectal dose and source strength for each patient. (A) International Commission on Radiation Units and Measurements Report 38 rectal reference point ($ICRU_{RP}$). (B) D_{2cc}. (C) D_{1cc}. (D) $D_{0.1cc}$.

and rectal BED on rectal complications after HDR-ICBT in patients with uterine cervical carcinoma. However, the previous study had a limitation in that we had defined the rectal dose as the dose to the lead wire inserted into the rectal lumen, which made it difficult to compare our result with those of other reports. We therefore decided this time to calculate the rectal dose by using the $ICRU_{RP}$ or GEC-ESTRO DVH parameters, which are considered to represent generally accepted dose points or parameters for communicating results among institutions. For the current study, the establishment of four groups of patients by using threshold levels for the rectal dose (≥ or <median dose) and source strength (≥ or <2.4 cGy.m^2.h^{-1}) showed that patients with values above the respective thresholds experienced a significantly greater frequency of rectal bleeding than did other patients. It should be noted that patients with a rectal median dose above the threshold did not show a greater frequency of rectal bleeding unless the source strength exceeded 2.4 cGy.m^2.h^{-1}. These results are in agreement with those reported by the previous study. These findings together suggest that rectal bleeding is affected not only by rectal dose but also by ^{192}Ir source strength during HDR-ICRT.

Table 3. Correlation of clinical factors with rectal bleeding

Factor	Patients, *n*	Rectal bleeding, *n* (%)		*p**
		No	Yes	
Age (y)				0.85
<70	32	24 (75)	8 (25)	
≥70	30	21 (70)	9 (30)	
Local stage				0.89
I–II	37	26 (70)	11 (30)	
III–IV	25	19 (76)	6 (24)	
CCRT				0.17
No	37	29 (78)	8 (22)	
Yes	25	16 (64)	9 (36)	

Abbreviation: CCRT = concurrent chemoradiotherapy.
* Log–rank test.

Figure 2 shows that the source strength is not the only prognostic factor for rectal bleeding (p = 0.08). For $D_{0.1cc}$ (which would correspond to the maximal dose as determined by X-ray–based planning), there was no significant difference in rectal bleeding between Group 4 (≥median dose and ≥2.4 cGy.m^2.h^{-1}) and Group 3 (≥median dose and <2.4 cGy.m^2.h^{-1}) (Fig. 3). These data indicate that the rectal dose is a more powerful prognostic factor for rectal bleeding than is the source strength.

In our previous study, the rectal dose was calculated as the BED by combining the EBRT and the HDR dose. In the current study, rectal dose is shown as the EQD_2 dose for reasons of simplicity and to allow for correlation with standard low-dose-rate (LDR) doses. The median EQD_2 values were 65 Gy

for $ICRU_{RP}$ and 71 Gy for D_{2cc}, which correspond to a BED Gy_3 of 107 Gy and 119 Gy, respectively. These values are a little higher than those of our earlier results using data obtained by inserting a lead wire into the rectal lumen (with a median BED of 101.5 Gy_3), because the lead wire in the lumen tends to separate from the rectal wall and thus to result in underestimation of the rectal wall dose as confirmed in the cohort of the present study (data not shown).

These days, conventional $ICRU_{RP}$ is not always considered to be the best predictor of rectal dose (9). However, there are a few reports of $ICRU_{RP}$ correlating well with D_{2cc} in a CT-based DVH analysis (10, 11). Additionally, GEC-ESTRO has recommended both $ICRU_{RP}$ and DVH parameters for recording and reporting because the correlation between dose–volume relations and dose–volume effect has scarcely been investigated (7). We therefore decided to analyze rectal dose by using both $ICRU_{RP}$ and CT-based DVH parameters. Many studies using $ICRU_{RP}$ (12, 13) or DVH parameters in HDR-ICBT have indicated that a higher rectal dose is significantly related with rectal bleeding. Noda *et al.* (14), using a CT-based rectal mucosal point dose, showed that a rectal BED ≥ 140 Gy_3 was associated with a significantly greater frequency of rectal complications, and Koom *et al.* (15) found that several DVH parameters obtained from three-dimensional CT-based treatment planning or $ICRU_{RP}$ are significantly associated with endoscopic scoring of mucosal changes in the rectum. However, these reports of CT-based DVH analysis results show only the relationship between rectal dose and rectal bleeding but do not deal with the power of the source.

The dose–rate effect has been analyzed in several LDR studies, which have shown that a higher dose–rate is associated with a higher incidence of late morbidity (16, 17). Therefore, we hypothesized that a higher dose–rate is also correlated with a higher incidence of rectal bleeding in ^{192}Ir HDR-ICBT. However, it is difficult to evaluate the dose–rate effect in ^{192}Ir HDR-ICBT compared with LDR-ICBT because the ^{192}Ir source has a short half-life (about 74 days) and attenuates rapidly during the treatment period (intra- or inter-fraction). In as much as the strength of the source is thought to affect the dose–rate, the ^{192}Ir source strength was measured on each day of the HDR-ICBT session, and the average source strength was calculated over three or four sessions as an indicator of the dose–rate.

The dose–rate effect at HDR is thought to be smaller than that at LDR because there is little impact of sublethal damage repair. However, the dose–rate effect at HDR is more complicated than at LDR because fractionation compensates for the relative lack of protection of late-responding normal tissues. An effect of dose–rate in HDR brachytherapy has been found in radiobiologic models (18, 19). Manning *et al.* (18) estimated the dose–rate effect using a single-plane template model, with examination of variability in dose–rate in brachytherapy performed with an HDR stepping source. Different late adverse effects were found between the relatively uniformly irradiated central zone of the template and the heterogeneously irradiated peripheral zone. The model also showed pronounced dependence on source strength, especially in cells of late-responding tissues with short repair times. In HDR treatment of cervical carcinoma using a stepping source, the instant dose–rate at each stepping point (dwell point) changes dramatically during the time course of irradiation. A peripheral location of the applicator, such as the rectal wall, may provide irradiation at an ultra-high dose–rate. Positioning of the source at the ovoid apex is likely to provide a higher dose–rate and a higher source strength, and it is likely to be associated with a late rectal effect.

One weakness of this study is that CT scans after insertion of an applicator were obtained only during the first HDR-ICRT session. However, the occurrence between sessions of substantial changes in the spatial relationship of the applicator relative to target structures and OARs have been demonstrated (20, 21), and these findings indicate the importance of individual treatment planning for each fraction. Examination of pelvic CT images for every ICBT session would allow precise calculation of dose parameters, but this approach would be time consuming and not cost effective in actual practice. The GEC-ESTRO group has provided recommendations for target delineation using MRI-contoured volumes (6, 7). MRI is superior to CT for imaging the normal anatomy of the female pelvis and for identifying the extent of cervical carcinoma, but we were unable to perform MRI scans during ICBT because of the lack of an MRI-specific applicator. Viswanathan *et al.* (22) reported that CT tumor contours can overestimate the tumor volume but that there were no significant differences between CT and MRI in terms of volumes or doses to the OARs. We therefore believe that CT-based contouring is adequate for DVH analysis of OARs.

In conclusion, this is the second report on evaluation of the effect of ^{192}Ir source strength on rectal bleeding in patients undergoing HDR-ICRT. Our results show that both rectal dose and source strength affect rectal bleeding after HDR-ICRT using $ICRU_{RP}$ and CT-based DVH parameters.

REFERENCES

1. Lanciano RM, Martz K, Coia LR, *et al.* Tumor and treatment factors improving outcome in stage III-B cervix cancer. *Int J Radiat Oncol Biol Phys* 1991;20:95–100.
2. Montana GS, Fowler WC, Varia MA, *et al.* Carcinoma of the cervix, stage III. Results of radiation therapy. *Cancer* 1986; 57:148–154.
3. Nag S, Orton C, Young D, *et al.* The American brachytherapy society survey of brachytherapy practice for carcinoma of the uterine cervix in the United States. *Gynecol Oncol* 1999;73: 111–118.
4. Toita T, Kodaira T, Shinoda A, *et al.* Patterns of radiotherapy practice for patients with cervical cancer (1999-2001): Patterns of care study in Japan. *Int J Radiat Oncol Biol Phys* 2008;70: 788–794.
5. Suzuki O, Yoshioka Y, Isohashi F, *et al.* Effect of high-dose-rate ^{192}Ir source activity on late rectal bleeding after

intracavitary radiation therapy for uterine cervical cancer. *Int J Radiat Oncol Biol Phys* 2008;71:1329–1334.

6. Haie-Meder C, Pötter R, Van Limbergen E, *et al.* Recommendations from Gynaecological (GYN) GEC-ESTRO Working Group (I): Concepts and terms in 3D image based 3D treatment planning in cervix cancer brachytherapy with emphasis on MRI assessment of GTV and CTV. *Radiother Oncol* 2005;74:235–245.
7. Pötter R, Haie-Meder C, Van Limbergen E, *et al.* Recommendations from gynaecological (GYN) GEC ESTRO working Group (II): Concepts and terms in 3D image-based treatment planning in cervix cancer brachytherapy-3D dose volume parameters and aspects of 3D image-based anatomy, radiation physics, radiobiology. *Radiother Oncol* 2006;78:67–77.
8. Fowler JF. The linear-quadratic formula and progress in fractionated radiotherapy. *Br J Radiol* 1989;62:679–694.
9. Hoskin PJ, Bownes P. Innovative technologies in radiation therapy: brachytherapy. *Semin Radiat Oncol* 2006;16:209–217.
10. van den Bergh F, Meertens H, Moonen L, van Bunningen B, *et al.* The use of a transverse CT image for the estimation of the dose given to the rectum in intracavitary brachytherapy for carcinoma of the cervix. *Radiother Oncol* 1998;47:85–90.
11. Pelloski CE, Palmer M, Chronowski GM, *et al.* Comparison between CT-based volumetric calculations and ICRU reference-point estimates of radiation doses delivered to bladder and rectum during intracavitary radiotherapy for cervical cancer. *Int J Radiat Oncol Biol Phys* 2005;62:131–137.
12. Ogino I, Kitamura T, Okamoto N, *et al.* Late rectal complication following high dose rate intracavitary brachytherapy in cancer of the cervix. *Int J Radiat Oncol Biol Phys* 1995;31:725–734.
13. Clark BG, Souhami L, Roman TN, *et al.* The prediction of late rectal complications in patients treated with high dose-rate brachytherapy for carcinoma of the cervix. *Int J Radiat Oncol Biol Phys* 1997;38:989–993.
14. Noda SE, Ohno T, Kato S, *et al.* Late rectal complications evaluated by computed tomography-based dose calculations in patients with cervical carcinoma undergoing high-dose-rate brachytherapy. *Int J Radiat Oncol Biol Phys* 2007;69:118–124.
15. Koom WS, Sohn DK, Kim JY, *et al.* Computed tomography-based high-dose-rate intracavitary brachytherapy for uterine cervical cancer: Preliminary demonstration of correlation between dose-volume parameters and rectal mucosal changes observed by flexible sigmoidoscopy. *Int J Radiat Oncol Biol Phys* 2007;68:1446–1454.
16. Lambin P, Gerbaulet A, Kramar A, *et al.* Phase III trial comparing two low dose rates in brachytherapy of cervix carcinoma: Report at two years. *Int J Radiat Oncol Biol Phys* 1993;25: 405–412.
17. Haie-Meider C, Kramar A, Lambin P, *et al.* Analysis of complications in a prospective randomized trial comparing two brachytherapy low dose rates in cervical carcinoma. *Int J Radiat Oncol Biol Phys* 1994;29:953–960.
18. Manning MA, Zwicker RD, Arthur DW, *et al.* Biologic treatment planning for high-dose-rate brachytherapy. *Int J Radiat Oncol Biol Phys* 2001;49:839–845.
19. Smina P, Schneider CJ, Fowler JF. The optimal fraction size in high-dose-rate brachytherapy: Dependency on tissue repair kinetics and low-dose-rate. *Int J Radiat Oncol Biol Phys* 2002;52:844–849.
20. Jones ND, Rankin J, Gaffney DK. Is simulation necessary for each high-dose-rate tandem and ovoid insertion in carcinoma of the cervix? *Brachytherapy* 2004;3:120–124.
21. Kirisits C, Lang S, Dimopoulos J, *et al.* Uncertainties whenusing only one MRI-based treatment plan for subsequent high-dose-rate tandem and ring applications in brachytherapy of cervix cancer. *Radiother Oncol* 2006;81:269–275.
22. Viswanathan AN, Dimopoulos J, Kirisits C, *et al.* Computed tomography versus magnetic resonance imaging-based contouring in cervical cancer brachytherapy: Results of a prospective trials and preliminary guidelines for standardized contours. *Int J Radiat Oncol Biol Phys* 2007;68:491–498.

Original Article

Postoperative Radiation Therapy After Complete Resection of Thymoma Has Little Impact on Survival

Tomoki Utsumi, MD, PhD[1]; Hiroyuki Shiono, MD, PhD[1]; Yoshihisa Kadota, MD, PhD[1]; Akihide Matsumura, MD, PhD[2]; Hajime Maeda, MD, PhD[3]; Mitsunori Ohta, MD, PhD[4]; Yasuo Yoshioka, MD, PhD[5]; Masahiko Koizumi, MD, PhD[5]; Takehiro Inoue, MD, PhD[5]; and Meinoshin Okumura, MD, PhD[1]

BACKGROUND: Postoperative radiation therapy for thymoma is widely used, although the clinical benefits are controversial. Furthermore, to the authors' knowledge, the relation between postoperative radiation therapy and cell type classified by the World Health Organization (WHO) is not known. **METHODS:** The records of 324 patients (ages 17-83 years; mean, 51 years; 160 males and 164 females) who underwent complete resection of a thymoma between 1970 and 2005 were reviewed. Mediastinum postoperative radiation therapy was performed for 134 patients. Survival rates and patterns of recurrence were determined according to Masaoka stage and WHO cell type. **RESULTS:** The 10-year disease-specific survival rates for patients with and without postoperative radiation therapy were 92.8% and 94.4%, respectively ($P = .22$). Subset analyses after stratifying by Masaoka stage and WHO cell type demonstrated that the 10-year disease-specific survival rate for patients without postoperative radiation therapy with Masaoka stage I and II, as well as those with WHO cell types A, AB, or B1, was 100%, which was satisfactory. Furthermore, the rates for patients with Masaoka stage III/IV and those with WHO cell types B2/B3 with or without postoperative radiation therapy were not found to be significantly different. In 24 patients with disease recurrence, pleural dissemination was observed most often, followed by distant metastases; local disease recurrence without other recurrence occurred in 2. **CONCLUSIONS:** The authors concluded that surgical resection alone is sufficient for thymoma patients with Masaoka stage I and II, and those with WHO cell types A, AB, and B1. Furthermore, an optimal treatment strategy should be established for patients with Masaoka stage III/IV and WHO cell type B2/B3 thymomas. **Cancer 2009;115:5413-20. © 2009 American Cancer Society.**

KEY WORDS: thymoma, surgery, radiation therapy, complete resection, survival, Masaoka stage, World Health Organization histologic classification.

When classifying the advancement of thymomas, the Masaoka staging system[1,2] has been widely used because it is a good predictor of prognosis for those patients,[3] in addition to its clarity in assigning patients to an appropriate stage. Conversely, thymomas are also histologically classified based on a system proposed in 1999 and revised in 2004 by the World Health Organization (WHO).[4] In that classification, which is also

Corresponding author: Tomoki Utsumi, MD, PhD, Department of General Thoracic Surgery, Osaka University Graduate School of Medicine, 2-2 (L-5), Yamadaoka, Suita, Osaka 565-0871, Japan; Fax: (011) 81-6-6879-3164; utsumi@thoracic.med.osaka-u.ac.jp

[1]Department of General Thoracic Surgery, Osaka University Graduate School of Medicine, Suita, Japan; [2]Department of Surgery, National Hospital Organization Kinki-Chuo Chest Medical Center, Sakai, Japan; [3]Department of Surgery, Toneyama National Hospital, Toyonaka, Japan; [4]Department of General Thoracic Surgery, Osaka Prefectural Medical Center for Respiratory and Allergic Diseases, Habikino, Japan; [5]Department of Radiation Oncology, Osaka University Graduate School of Medicine, Suita, Japan

Received: November 6, 2008; **Revised:** April 29, 2009; **Accepted:** May 4, 2009

Published online August 14, 2009 in Wiley InterScience (www.interscience.wiley.com)

DOI: 10.1002/cncr.24618, www.interscience.wiley.com

considered to compose another prognostic factor independent of Masaoka stage,[5-7] thymomas are divided into 5 types; A, AB, B1, B2, and B3.

Although to our knowledge no randomized controlled trial has been conducted to date to establish a standard treatment for a thymoma, empiric evidence has led surgical resection to become the mainstay therapy. However, thymomas are also sensitive to radiation therapy (RT), which is often used in nonresectable patients and after surgery as an adjuvant therapy. The impact of postoperative RT on survival after complete resection of a thymoma has been reported in several reports, although the results vary.[8-15] All of those reports used Masaoka stage to stratify their patients; however, to our knowledge, no known correlations between the effects of postoperative RT and WHO cell type have been presented to date. We conducted the current retrospective study to determine whether certain patients with a thymoma could achieve prolonged survival by receiving postoperative RT after a complete resection, by stratifying the patients according to Masaoka stage and WHO cell type. The relation between RT status and pattern of disease recurrence was also examined to investigate the effects of RT on the clinical course of thymoma patients.

MATERIALS AND METHODS

We reviewed the records of 324 patients who underwent complete resection of a thymoma at Osaka University Hospital and its affiliated hospitals during the 36-year period between 1970 and 2005. Those with a final diagnosis of thymic carcinoma and those who underwent a biopsy alone were not included. The patients included 160 males and 164 females, who ranged in age from 17 to 83 years (mean, 51 years). Postoperative RT was initially recommended for all patients who underwent a complete resection; however, it was not performed in cases of patient refusal. In addition, the criteria for postoperative RT at Osaka University Hospital changed during the study period, that is, Masaoka stage I patients were first eliminated from this recommendation in 1985, followed by stage II patients in 1998. Conversely, postoperative RT was not always recommended to patients at other hospitals that participated in this study. As a result, 134 patients received postoperative RT, of whom 119 were treated at Osaka University Hospital.

Postoperative RT was administered using megavoltage technology. Cobalt-60 and 6-megavolt (MV) x-ray devices were used from 1970 through 1981; cobalt-60 and 10-MV x-ray devices were used from 1982 through 1993; and 4-MV, 6-MV, and 10-MV x-ray devices were used from 1993. In 1997, evaluation of dose distribution using computed tomographic images and 3-dimensional planning became available (n = 20). The typical volume treated included the entire tumor bed and part of the involved adjacent lung when there was parenchymal involvement or as delineated by surgical clips, with at least a 1.5-cm margin. For some patients, the entire mediastinum was included in the treatment field, whereas noninvolved supraclavicular fossa was never included. Treatment portals included opposing anterior-posterior fields with differential weighting (1:1, 3:2, 2:1, 3:1) or a single anterior field. For all patients, a total dose of 40 to 50 grays (Gy) with 2 Gy per fraction was intended, although the RT course could not be completed in 12 patients. We adopted in principle 40 Gy, which adhered fundamentally to the recommendation stated in a study performed at our former institute.[9] Thus, 84% of the patients in the postoperative RT group received a dose of 40 Gy (median, 40 Gy; average, 39.3 Gy [range, 10-50 Gy]).

Patient characteristics in regard to Masaoka stages and other perioperative therapy with reference to the status of postoperative RT are summarized in Table 1. Actuarial disease-specific and overall survival rates for all patients and those in each stage were calculated after dividing them by the status of postoperative RT. As we previously reported, the survival rates of patients with a stage III thymoma were found to be correlated with the involved organs.[3] Therefore, stage III patients were divided into 3 groups according to the involved organs: those with invasion to the great vessels (V[+]L[+ or −]P[+ or −]), invasion to the lung but not the great vessels (V[−]L[+]P[+ or −]), and invasion to the pericardium but not the great vessels or lungs (V[−]L[−]P[+]).

Pathologic examinations were performed using hematoxylin and eosin-stained sections derived from paraffin-embedded blocks. Histologic diagnosis with reference to the WHO classification system was performed to classify the patients according to cell type A, AB, B1, B2, or B3, which was identified in 290 patients. Actuarial survival rates were calculated, and patterns of disease recurrence were reviewed based on each cell type.

Table 1. Patient Characteristics According to Postoperative RT Status

Postoperative RT	Yes	No
Masaoka stage		
I	31	119
II	43	33
III	53	30
IVA	4	5
IVB	3	3
Total	134	190
Preoperative therapy	6	25
RT	2	9
Chemotherapy	4	10
Steroids	2	11
Postoperative therapy other than RT	17	18
Chemotherapy	8	5
Steroids	12	13

RT indicates radiation therapy.

When considering the clinical course of a patient with a thymoma, which lasts for more than a decade in many, disease-specific survival rates may accurately reflect the clinical course of thymomas as compared with overall survival rates. Therefore, both disease-specific and overall survival rates were calculated in the current study. Patients who died from a disease other than the thymoma were regarded as censored at the time of death in treating disease-specific survival rates. Actuarial disease-specific and overall survival rates were calculated using the Kaplan-Meier method, and statistical differences between survival curves were examined with a log-rank test. The frequencies of distribution between groups were tested with a chi-square test. A P value of $<.05$ was considered significant. Statistical analyses were performed using the personal computer software package StatView 5 (SAS Institute, Cary, NC). The institutional review board of Osaka University Hospital approved the design of the study and consented to waive the need to obtain informed consent from the patients.

RESULTS

The actuarial 10-year and 20-year disease-specific survival rates for patients who received postoperative RT were 92.8% and 83.5%, respectively, whereas they were 94.4% and 94.4%, respectively, for those treated without RT ($P = .2208$). Conversely, the actuarial 10-year and 20-year overall survival rates for those who received postoperative RT were 80.7% and 56.5%, respectively, whereas they were 86.2% and 40.4%, respectively, for those treated without RT ($P = .0640$). The distribution of patients in regard to Masaoka stage was skewed in the present population, thus disease-specific and overall survival rates for the patients were calculated by stage (Table 2). The disease-specific survival rate for patients with stage I and II was >90% regardless of the status of postoperative RT. Furthermore, in all patients with stage III disease, there were no significant differences noted in disease-specific survival rate between those treated with and without postoperative RT (Table 2). Next, we compared stage III patients after dividing them according to the involved organs. The actuarial 10-year and 20-year disease-specific survival rates for patients in the V(+)L(+ or −)P(+ or −) group who underwent postoperative RT (n = 12) were 62.3% and 41.6%, respectively, whereas they were 77.1% and 77.1%, respectively, for those treated without RT (n = 13; $P = .48$). Similarly, those rates for the V(−)L(+)P(+ or −) group treated with postoperative RT (n = 27) were 93.8% and 54.8%, respectively. Although the follow-up period for those treated without postoperative RT in this group (n = 12) was not adequate to calculate the 10-year disease-specific survival rate, the disease-specific survival rate after 9 years was 80.0% ($P = .2565$). No patients in the V(−)L(−)P(+) group died during the follow-up period of between 1.8 to 20.6 years (median, 9.9 years), which included 14 patients treated with postoperative RT and 5 treated without it. In patients with stage IVA disease, all 5 patients without postoperative RT and 3 of 4 patients with postoperative RT survived >5 years, whereas the remaining 1 patient with postoperative RT died 1.4 years after surgery. With regard to those with stage IVB disease, all 6 died within 5 years.

The overall survival rate for patients with stage I and II disease without postoperative RT was >90%, whereas it was smaller in those treated with postoperative RT compared with those treated without. Furthermore, in all patients with stage III disease, there were no significant differences in the overall survival rate noted between those treated with and without postoperative RT. With regard to patients with stage IV disease, all deaths that occurred were because of the tumor, thus, the overall survival rates were identical to the disease-specific survival rates, which were analyzed above (Table 2).

Table 2. Patient Survival Rate Based on Masaoka Stage

Stage	Postop RT	No.	10DSR, %	20DSR, %	*P*	10OSR, %	20OSR, %	*P*
I	+	31	96.3	90.3		77.3	58.7	
	–	119	100	100	NA	92.3		.0126
II	+	43	100	100		85.0	73.6	
	–	33	100		NA	96.7		.2486
III	+	53	87.7	62.3		79.9	35.5	
	–	30	85.1	85.1	.8010	69.1	46.1	.4852
IV	+	7	62.5 (5DSR)			62.5 (5OSR)		
	–	8	66.7 (5DSR)		.6628	66.7 (5OSR)		.6628

Postop RT indicates postoperative radiation therapy; 10DSR, 10-year disease-specific survival rate; 20DSR, 20-year disease-specific survival rate; 10OSR, 10-year overall survival rate; 20OSR, 20-year overall survival rate; +, received; –, not received; NA, not applicable; 5DSR, 5-year disease-specific survival rate; 5OSR, 5-year overall survival rate.

Table 3. Survival Rates and Patterns of Disease Recurrence According to WHO Cell Type

WHO Cell Type	Postop RT	Masaoka Stage					Total	10DSR, %	20DSR, %	10OSR, %	20OSR, %	Patten of Disease Recurrence
		I	II	III	IVA	IVB						
A	+	2		1			3	100	100	66.7	66.7	None
	–	12	1	1			14	100	—	100	—	None
AB	+	9	12	5		2	28	92.4	84.0	88.9	66.6	PD (2), local, unknown
	–	47	15	1		1	64	100	—	85.1	—	None
B1	+	6	10	3			19	100	100	88.8	66.0	PD
	–	25	5	5			35	100	—	90.5	—	None
B2	+	10	12	25	3	1	51	94.9	73.9	76.5	48.3	PD (8), lung, local, brain, and pericard
	–	21	6	12	5	1	45	92.9	92.9	82.5	41.3	Lung and PD (2)
B3	+		7	4	1		12	88.9	—	67.9	—	PD + local + liver, local + lung, and PD + lung
	–	4	3	3		1	11	65.6	—	65.6	—	Lung
Others*	+						0					
	–	6	1	1			8					
Total		142	72	61	9	6	290					

WHO indicates World Health Organization; Postop RT, postoperative radiation therapy; 10DSR, 10-year disease-specific survival rate; 20DSR, 20-year disease-specific survival rate; 10OSR, 10-year overall survival rate; 20OSR, 20-year overall survival rate; +, received; –, not received; PD, pleural dissemination, pericard, pericardial dissemination.

* "Others" in WHO cell type includes cases that could not be assigned to type A, AB, B1, B2, or B3.

The distribution by WHO cell type according to Masaoka stage and status of postoperative RT for each category is summarized in Table 3. None of the patients with WHO cell types A (n = 17) or B1 (n = 54) died during the median follow-up period of 5.4 years and 8.3 years, respectively, regardless of the status of postoperative RT. Furthermore, no patient of disease recurrence occurred in cases with cell type A, whereas 1 patient with cell type B1 developed disease recurrence with pleural dissemination, which had been classified as stage III disease at the time of resection and the patient received postoperative RT. Among those with cell type AB (n = 92), 3 patients treated with postoperative RT died at 1.5 years, 3.8 years, and 16.7 years, respectively, after surgery, whereas no patient treated without postoperative RT died. Patterns of disease recurrence were found in 1 patient with pleural and pericardial dissemination, 1 with pleural dissemination and lymph node metastasis, and 1 with disease recurrence at the site of a needle biopsy. The actuarial 10-year and 20-year disease-specific survival rates for all patients with these 3 cell types who underwent postoperative RT (n = 50) were 95.8% and 91.5%, respectively, whereas the 15-year disease-specific survival rate for those treated without postoperative RT was 100% (n = 113).

Of 96 patients with WHO cell type B2, 8 died, which included 6 with stage III disease and 2 with stage IVA disease. All but 1 of the patients who died received postoperative RT. There was no significant difference noted with regard to actuarial disease-specific survival rate between patients treated with and those treated without postoperative RT ($P = .4368$) (Table 3). Disease recurrence occurred in 16 patients, which included 1 patient with stage II disease, 11 patients with stage III disease, and 4 patients with stage IVA disease, with postoperative RT performed in 13 of those. The pattern of disease recurrence in most included pleural or pericardial dissemination and distant metastases. Local disease recurrence without the existence of other recurrent disease occurred in 1 patient with stage III disease who underwent postoperative RT.

Among patients with WHO cell type B3, 3 died from the thymoma, 2 of whom received postoperative RT. No significant difference in actuarial disease-specific survival rates were found between those treated with and without postoperative RT ($P = .3501$). Disease recurrence occurred in 4 patients, which included 2 with stage III, and 1 each with stage IVA and stage IVB disease, with postoperative RT performed in 3 of those. The patterns of disease recurrence included pleural dissemination, distant metastases in the liver and lung, and local disease recurrence. Local disease recurrence accompanied by distant metastasis occurred in 2 patients.

No group of patients divided by WHO cell type demonstrated a significant difference in overall survival rate according to status of postoperative RT ($P = .7496$, .9634, .1837, and .7229 for WHO cell types AB, B1, B2, and B3, respectively) (Table 3). Statistical analysis of overall survival rates for patients with WHO cell type A was not attempted because no events occurred in those patients treated without postoperative RT, and the number of patients treated with postoperative RT was too small.

DISCUSSION

In the current study, no significant improvement in survival was noted for patients who were treated with postoperative RT compared with those without, regardless of Masaoka stage, which is consistent with previously reported results.[10-16] With regard to those with Masaoka stage I and II disease, the results of the current study can be explained in part by the finding that the long-term outcomes of our thymoma patients who did not undergo postoperative RT were satisfactory, which made it difficult to demonstrate that postoperative RT had a further benefit on survival, thus suggesting that complete resection alone was sufficient to achieve a good prognosis in this population. Although the survival rates of stage III and IV disease patients were reduced compared with those with stage I and II, the differences in survival according to status of postoperative RT among each stage were not found to be significant, which may indicate that postoperative RT after complete resection in patients with stage III and IV disease does not alter long-term survival.

The indication of postoperative RT for thymoma after complete resection has long been considered controversial, mainly because, to the best of our knowledge, no randomized controlled study has been conducted to date. For patients with stage II and III disease, Curran et al.[8] and Nakahara et al.[9] advocated postoperative RT. Curran et al.reviewed 19 patients with stage II disease and 7 with stage III disease, and their findings supported postoperative RT for stage II disease based on their finding that mediastinal recurrence occurred in 6 of 18 patients treated without RT within 5 years, whereas no recurrence was noted in 1 stage II case and 4 stage III patients treated with postoperative RT. The mediastinum was the most common site of disease recurrence in their report. In addition, reports on the outcome of patients with a thymoma have been accumulating,[7,11,12,14,16,17] which led us to speculate regarding the effects of postoperative RT on stage II thymomas. Those reports studied from 25 to 61 patients with stage II disease, and noted a low rate of disease recurrence (range, 2.0-9.8%), with a frequent pattern of disease recurrence being pleural dissemination, which is consistent with the findings in the current study. Although this issue would ideally be settled by a prospective randomized controlled study, we consider that the accumulated data are sufficient to judge that postoperative RT for stage II thymoma is not effective.

Conversely, Nakahara et al insisted that a patient with a stage III thymoma should undergo postoperative RT for the entire mediastinum after a complete resection.[9] That report, produced by our former institute, was based on a 1-arm observation study that did not include patients who did not undergo postoperative RT. Later,

after accumulating clinical data for an additional 20 years, we reported that the prognosis and pattern of disease recurrence in patients with a stage III thymoma depended on the involved organs, and that recurrence was most often noted as pleural dissemination.[3,18] Thus, we currently consider that establishment of a strategy against pleural dissemination, rather than mediastinal recurrence, is more important than postoperative RT for this group of patients, as described earlier. To the best of our knowledge, no beneficial effect of postoperative RT on the survival of individuals with stage III thymoma has been demonstrated to date in reports published from other institutions,[11,15] which is consistent with the results of the current study.

Long-term survival rates for patients with WHO cell types A, AB, and B1 were considered adequate without postoperative RT, making it difficult to demonstrate further improvement because of postoperative RT and suggesting that its role was not apparent in this population, which indicates that surgery alone is a sufficient treatment strategy for thymoma patients with WHO cell types A, AB, and B1, as well as those classified as having Masaoka stage I and II disease who undergo a complete resection. Thus, such patients may be eliminated as candidates for postoperative RT. Furthermore, of the 56 patients in the current study classified as having stage III, IVA, or IVB disease, and WHO cell types B2 or B3, 37 were Masaoka stage III and WHO cell type B2, and there was no significant difference in survival noted with regard to the status of postoperative RT among them (data not shown). The other combinations included no more than 8 patients, which was not considered to be a sufficient number with which to demonstrate the effect of RT on long-term survival.

Patterns of disease recurrence are another issue regarding postoperative therapy for patients with completely resected thymomas. The irradiation area in the patients in the current study was the mediastinum, which may function as a prophylactic against local recurrence of the tumor. The most frequent pattern of disease recurrence was pleural dissemination, followed by distant metastasis, mainly in the lungs. However, that phenomenon was common in patients who were treated both with and without postoperative RT and thus it does not appear that postoperative RT to the mediastinum prevents local recurrence. Other reports have also noted that the pleura is the most frequent site of recurrence,[11,15,19] and that performance of postoperative RT does not affect the rate of pleural recurrence.[11] Therefore, it would be reasonable to form a strategy against pleural dissemination and distant metastasis, rather than local control in the mediastinum, for thymomas that may require treatment in addition to complete resection. Some investigators have reported reductions in disease recurrence rates after entire hemithorax RT of approximately 15 Gy as adjuvant therapy after complete resection of a thymoma.[20,21] However, they also noted that radiation pneumonitis of grade 2 or greater occurred in 15% to 25% of those patients who underwent entire hemithorax RT, which led us to consider that this treatment should not be routine. In this context, systemic chemotherapy may be a good candidate modality. Although we could not find any reports in literature indicating that adjuvant chemotherapy after complete resection would ameliorate the outcome, there are studies describing favorable effects of systemic chemotherapy for patients with advanced thymomas. Various therapeutic regimens were used in those, including the quadruplet of doxorubicin, cisplatin, vincristine, and cyclophosphamide[22] and triplets of cisplatin, doxorubicin, and cyclophosphamide[23]; cisplatin, doxorubicin, and cyclophosphamide[24]; cisplatin, epirubicin, and etoposide[24,25]; and cisplatin, doxorubicin, and methylprednisolone,[26] as well as others. Because to our knowledge there is no standard chemotherapeutic protocol for a thymoma, it is important to determine the most suitable regimen as well as establish a multimodality treatment strategy for patients with stage III/IV thymoma and WHO cell types B2/B3.

A limitation of the current study is its retrospective design. We clearly understand that it would be ideal for a sufficient number of patients to be recruited within a short period to form a prospective study; however, the relative rareness of the disease makes it quite difficult to do so. In addition, confirmation of the effects of treatments require a long period, because the clinical course of a thymoma is slow, making it difficult to perform prospective randomized clinical studies of affected individuals. Therefore, the distribution of patients in the current study in regard to RT status was not randomized. However, we are certain that the bias used for selecting patients who received postoperative RT was minimal, because we determined the criteria for postoperative RT based on Masaoka

stage, not on a "case-by-case" basis. Conversely, the majority of the patients who received postoperative RT underwent surgery at Osaka University Hospital, which might cause a bias from the differences among the hospitals in this study. Nevertheless, all thoracic surgeons who participated in the current study were trained under a system established by Osaka University Hospital and its affiliated hospitals, and we therefore are confident that quality of the surgical procedures as well as perioperative care was maintained at a high level. Another important issue in the current study may be the long duration required to accumulate an adequate number of patient records because of the rareness of the disease, as such a long period may skew the outcome of a retrospective study. Over the study period of several decades, many aspects of thymoma treatment have changed, such as application of thoracoscopic surgery, new apparatuses for RT, new chemotherapeutic agents, and improvements in radiographic imaging technologies. Any of those variations in the patients in the current study might have skewed our results.

In conclusion, the effects of postoperative RT on survival and disease recurrence after complete resection in patients with thymoma were examined based on Masaoka stage and WHO cell type. A good candidate group of thymoma patients could not be identified after dividing by Masaoka stage and WHO cell type. However, patients with stage I and II thymoma, as well as those with WHO cell types A, AB, and B1, can be eliminated from the list of candidates for postoperative RT. Conversely, establishment of an optimal treatment strategy for patients with Masaoka stage III and IV disease, and WHO cell types B2 and B3, is needed to further improve their long-term outcome.

Conflict of Interest Disclosures

The authors made no disclosures.

References

1. Masaoka A, Monden Y, Nakahara K, Tanioka T. Follow-up study of thymomas with special reference to their clinical stages. *Cancer.* 1981;48:2485-2492.
2. Yamakawa Y, Masaoka A, Hashimoto T, et al. A tentative tumor-node-metastasis classification of thymoma. *Cancer.* 1991;68:1984-1987.
3. Okumura M, Miyoshi S, Takeuchi Y, et al. Results of surgical treatment of thymomas with special reference to the involved organs. *J Thorac Cardiovasc Surg.* 1999;117:605-613.
4. Travis WD, Brambilla E, Muller-Hermelink HK, Harris CC. World Health Organization Classification of Tumours. Pathology and Genetics of Tumours of the Lung, Pleura, Thymus and Heart. Lyon, France: IARC Press; 2004.
5. Okumura M, Ohta M, Tateyama H, et al. The World Health Organization histologic classification system reflects the oncologic behavior of thymoma: a clinical study of 273 patients. *Cancer.* 2002;94:624-632.
6. Chen G, Marx A, Wen-Hu C, et al. New WHO histologic classification predicts prognosis of thymic epithelial tumors: a clinicopathologic study of 200 thymoma cases from China. *Cancer.* 2002;95:420-429.
7. Nakagawa K, Asamura H, Matsuno Y, et al. Thymoma: a clinicopathologic study based on the new World Health Organization classification. *J Thorac Cardiovasc Surg.* 2003; 126:1134-1140.
8. Curran WJ Jr, Kornstein MJ, Brooks JJ, Turrisi AT III. Invasive thymoma: the role of mediastinal irradiation following complete or incomplete surgical resection. *J Clin Oncol.* 1988;6:1722-1727.
9. Nakahara K, Ohno K, Hashimoto J, et al. Thymoma: results with complete resection and adjuvant postoperative irradiation in 141 consecutive patients. *J Thorac Cardiovasc Surg.* 1988;95:1041-1047.
10. Regnard JF, Magdeleinat P, Dromer C, et al. Prognostic factors and long-term results after thymoma resection: a series of 307 patients. *J Thorac Cardiovasc Surg.* 1996;112: 376-384.
11. Ogawa K, Uno T, Toita T, et al. Postoperative radiotherapy for patients with completely resected thymoma: a multi-institutional, retrospective review of 103 patients. *Cancer.* 2002;94:1405-1413.
12. Mangi AA, Wright CD, Allan JS, et al. Adjuvant radiation therapy for stage II thymoma. *Ann Thorac Surg.* 2002;74:1033-1037.
13. Kondo K, Monden Y. Therapy for thymic epithelial tumors: a clinical study of 1,320 patients from Japan. *Ann Thorac Surg.* 2003;76:878-884; discussion 84-85.
14. Singhal S, Shrager JB, Rosenthal DI, LiVolsi VA, Kaiser LR. Comparison of stages I-II thymoma treated by complete resection with or without adjuvant radiation. *Ann Thorac Surg.* 2003;76:1635-1641; discussion 41-42.
15. Mangi AA, Wain JC, Donahue DM, Grillo HC, Mathisen DJ, Wright CD. Adjuvant radiation of stage III thymoma: is it necessary? *Ann Thorac Surg.* 2005;79:1834-1839.
16. Rena O, Papalia E, Oliaro A, et al. Does adjuvant radiation therapy improve disease-free survival in completely resected Masaoka stage II thymoma? *Eur J Cardiothorac Surg.* 2007;31:109-113.
17. Kondo K, Yoshizawa K, Tsuyuguchi M, et al. WHO histologic classification is a prognostic indicator in thymoma. *Ann Thorac Surg.* 2004;77:1183-1188.

18. Utsumi T, Shiono H, Matsumura A, et al. Stage III thymoma: relationship of local invasion to recurrence. *J Thorac Cardiovasc Surg.* 2008;136:1481-1485.
19. Myojin M, Choi NC, Wright CD, et al. Stage III thymoma: pattern of failure after surgery and postoperative radiotherapy and its implication for future study. *Int J Radiat Oncol Biol Phys.* 2000;46:927-933.
20. Uematsu M, Yoshida H, Kondo M, et al. Entire hemithorax irradiation following complete resection in patients with stage II-III invasive thymoma. *Int J Radiat Oncol Biol Phys.* 1996;35:357-360.
21. Sugie C, Shibamoto Y, Ikeya-Hashizume C, et al. Invasive thymoma: postoperative mediastinal irradiation, and low-dose entire hemithorax irradiation in patients with pleural dissemination. *J Thorac Oncol.* 2008;3:75-81.
22. Fornasiero A, Daniele O, Ghiotto C, et al. Chemotherapy of invasive thymoma. *J Clin Oncol.* 1990;8:1419-1423.
23. Loehrer PJ Sr, Kim K, Aisner SC, et al. Cisplatin plus doxorubicin plus cyclophosphamide in metastatic or recurrent thymoma: final results of an intergroup trial. The Eastern Cooperative Oncology Group, Southwest Oncology Group, and Southeastern Cancer Study Group. *J Clin Oncol.* 1994;12:1164-1168.
24. Venuta F, Rendina EA, Longo F, et al. Long-term outcome after multimodality treatment for stage III thymic tumors. *Ann Thorac Surg.* 2003;76:1866-1872; discussion 72.
25. Lucchi M, Melfi F, Dini P, et al. Neoadjuvant chemotherapy for stage III and IVA thymomas: a single-institution experience with a long follow-up. *J Thorac Oncol.* 2006;1:308-313.
26. Yokoi K, Matsuguma H, Nakahara R, et al. Multidisciplinary treatment for advanced invasive thymoma with cisplatin, doxorubicin, and methylprednisolone. *J Thorac Oncol.* 2007;2:73-78.

Dose profile measurement using an imaging plate: Evaluation of filters using Monte Carlo simulation of 4 MV x-rays

Masatoshi Hashimoto,[1,2,a)] Tetsuya Tomita,[3] Koichi Sawada,[3] Toshioh Fujibuchi,[4] Teiji Nishio,[5] and Keiichi Nakagawa[1]

[1]*Division of Radiology and Biomedical Engineering, Graduate School of Medicine, The University of Tokyo, Bunkyo-ku, Tokyo 113-8655, Japan*

[2]*Department of Therapeutic Radiology, Medical Plaza Edogawa, Edogawa-ku, Tokyo 133-0052, Japan*

[3]*Department of Radiology, Chiba University Hospital, Cyuo-ku, Chiba 260-8677, Japan*

[4]*Department of Radiological Sciences, School of Health Science, Ibaraki Prefectural University, Inashiki-gun, Ibaraki 300-0394, Japan and Graduate School of Comprehensive Human Sciences, University of Tsukuba, Tsukuba-shi, Ibaraki 305-8575, Japan*

[5]*Particle Therapy Division, Research Center for Innovation Oncology, National Cancer Center Hospital East, Kashiwa-shi, Chiba 277-8577, Japan*

(Received 1 December 2008; accepted 1 March 2009; published online 7 April 2009)

Computed radiography (CR) is gradually replacing film. The application of CR for two-dimensional profiles and off-axis ratio (OAR) measurement using an imaging plate (IP) in a CR system is currently under discussion. However, a well known problem for IPs in dosimetry is that they use high atomic number (Z) materials, such as Ba, which have an energy dependency in a photon interaction. Although there are some reports that it is possible to compensate for the energy dependency with metal filters, the appropriate thicknesses of these filters and where they should be located have not been investigated. The purpose of this study is to find the most suitable filter for use with an IP as a dosimetric tool. Monte Carlo simulation (Geant4 8.1) was used to determine the filter to minimize the measurement error in OAR measurements of 4 MV x-rays. In this simulation, the material and thickness of the filter and distance between the IP and the filter were varied to determine most suitable filter conditions that gave the best fit to the MC calculated OAR in water. With regard to changing the filter material, we found that using higher Z and higher density material increased the effectiveness of the filter. Also, increasing the distance between the filter and the IP reduced the effectiveness, whereas increasing the thickness of the filter increased the effectiveness. The result of this study showed that the most appropriate filter conditions consistent with the calculated OAR in water were the ones with the IP sandwiched between two 2 mm thick lead filters at a distance of 5 mm from the IP or the IP sandwiched directly between two 1 mm lead filters. Using these filters, we measured the OAR at 10 cm depth with 100 cm source-to-surface distance and surface 10×10 cm^2 field size. The results of this measurement represented that it is possible to achieve measurements with less than within 2.0% and 2.0% in the field and with less than 1.1% and 0.6% out of the field by using 2 and 1 mm lead filters, respectively. © *2009 American Institute of Physics.* [DOI: 10.1063/1.3103572]

I. INTRODUCTION

For radiation therapy, it is important to measure the dose distribution in materials in order to put together a treatment plan that will give an accurate dose distribution and ensure that the dose to normal tissue is minimized. The usual way to measure this is to use an ion chamber in water as a gold standard. However, because this is a sort of point measurement, it is time-consuming to measure the off-axis ratio (OAR) in two or three dimensions. Furthermore, the resolution of scans is limited due to chamber size.

To measure the dose distribution with high spatial resolution the use of film is an easier solution.[1–4] However, the film needs to be developed, and requires that the film processor be maintained. With GafChromic film,[5–7] it may be much easier and more useful because of no need to be chemical processing; however, all facilities cannot afford to purchase the film digitizer and use such expensive films constantly as a quality assurance tool. On the other hand, computed radiography (CR) system,[8] which has been originally used for diagnostic purpose, has been more widely used than GafChromic film. Additionally, it is being discussed that CR becomes more prevalent in radiotherapy. The use of the film processor is decreasing.

A new dosimetric method using an imaging plate[9,10] (IP) in a CR system has recently been considered as a replacement for film,[11–13] with the advantage that this method does not need a film processor. However, IPs include high atomic number (high Z) materials such as barium, for which there is, in general, an energy dependency problem, which can produce an error in the measurements. It is reported that similar errors occur even in film measurements, but it is possible to

a)Electronic mail: m_hashimoto@movie.ocn.ne.jp.

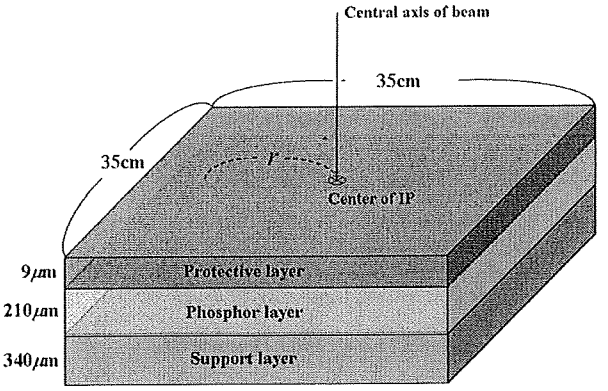

FIG. 1. Structure of the IP used in the MC simulation composed of three layers, a protective layer, a phosphor layer, and a support layer, respectively. r is the distance from the center of IP. The center of IP is corresponding to the central axis of x-ray.

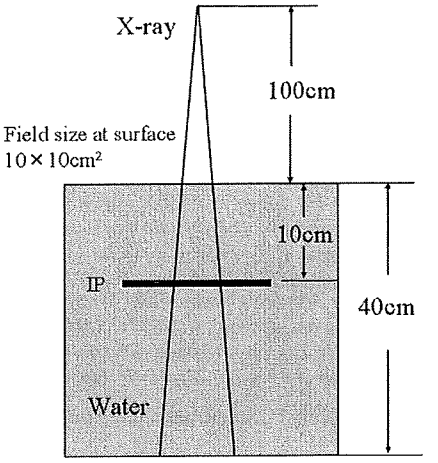

FIG. 2. Materials setting. A $40\times40\times40$ cm^3 water tank phantom was used in the simulation. The SSD was 100 cm and the field size 10×10 cm^2. The middle of water phantom was irradiated with a 4 MV photon beam. The incidence of photons was uniformly carried out in the exposure field. The IP was place at a depth of 10 cm from the surface of water.

compensate these errors with metal filters.[14–16] There has been a report asserting that filters can be used to compensate the errors for IP measurements also.[11] Nevertheless a detailed discussion regarding the kind of materials to use or where the filters should be placed, etc. has not taken place. The purpose of this study is to use Monte Carlo (MC) simulation to determine the most appropriate filter for IP measurements. In this investigation, we attempt to find the most appropriate material, thickness, and location of the filter for IP dosimetry in order to minimize the dosimetric error in OAR measurements with a 4 MV photon beam.

II. MATERIALS AND METHODS

A. MC simulation parameter settings and evaluation

For the MC simulations, we used GEANT4 (version 8.1 patch-01). GEANT4 is a calculation code widely used for high energy physics, nuclear physics, space physics, and medical physics, etc. The photon and electron interactions in the material are simulated down to 250 eV.[17] The GEANT4 physics models selected for this study were the low-energy electromagnetic process, and the number of history was 2×10^8 photons. GEANT4 utilizes a stopping range instead of energy to control the tracking and production of secondaries. In GEANT4, all particles are tracked to a zero range except for secondaries with a range shorter than the production cutoff range set by the user. In this study, the production cutoff range was set to 0.01 mm.

The spectrum used in this study was a 4 MV photon spectrum calculated from Schiff's formula.[18] There have been reports that this formula has been extended for medical linear accelerator.[19–21] In this study, we calculated the spectrum using Schiff's formula, where we attached 10 mm thick copper attenuations by every 50 keV as the target and the material under the target.

The IP used in the MC simulation is a ST-VN (FUJIFILM Corp., Minato-ku, Tokyo). As shown in Fig. 1 the size of the IP is $35\times35\times0.0559$ cm^3 and it is composed of three layers, a protective, phosphor, and support layer and protective and support layers are made of Polyethylene terephthalate (PET), and the phosphor layer is BaFBrI. The composition of PET is C:H:O=10:8:4 and the density is 1.38 g/cm^3. BaFBrI consists of 56.45% Ba, 7.81% F, 27.92% B, 7.82% I, and the density was set to 5.50 g/cm^3. To verify the calculation conditions, we compared measurements and simulation.

1. Measurement

The linear accelerator used was Clinac2100C (Varian Medical Systems Inc., Palo Alto, CA) and we used only 4 MV photons with a 10×10 cm^2 field and a 100 cm source-to-surface distance (SSD). For percentage depth dose (PDD) measurements in water, we used a PTW Freiburg N31005 ionization chamber in a three-dimensional (3D) water phantom (Dynascan, Computerized Medical Systems Inc., St. Louis, MO). We measured the PDD on the central beam axis and the OAR at a depth of 10 cm. For the OAR measurement with the IP, a 40×40 cm^2 water equivalent solid phantom (Solid Water Phantom, Gammex Inc., Middleton, WI) was used instead of the 3D water phantom. The IP (ST-VN, 35×35 cm^2, Fujifilm Corp., Minato-ku, Tokyo) was placed perpendicular to the beam axis at a depth of 10 cm in the stack of 40 cm solid phantom. The IP was exposed to a dose of 12.5 mGy, and was then read out using a FCR5000 (Fujifilm Medical Co. Ltd., Minato-ku, Tokyo) and converted to DICOM format where the S value, which gives the sensitivity of the FCR during read out, was set to 2, and the L value, which gives the latitude, was set to 4. The other parameter settings were S-Shift:1, C-Shift:1, GA:A, GC:1.2, GS:0.00, RN:3, RT: F, RE:0.0, and DRC: off. These values were all fixed. The OAR data were obtained from a line profile on the acquired two-dimensional IP dose profiles. To determine the dose deposited on the IP we made the dose conversion table for the pixel value on the IP. First we measured at the central axis with an ion chamber from 2.5 to 15 mGy under the same condition, and next we read out the

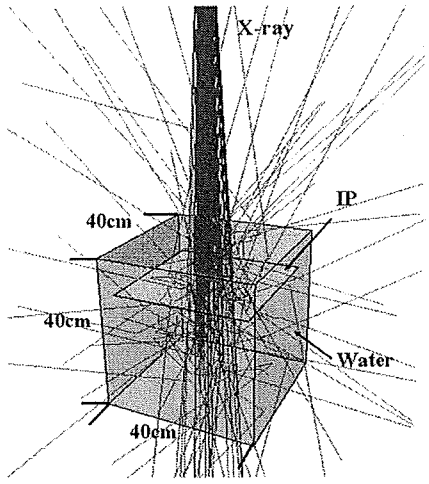

FIG. 3. Example showing the behavior of 100 photons in the water phantom.

corresponding data area on the IP, 100×100 pixels with each pixel being 0.1×0.1 mm^2, and which was compared with the one with ion chamber.

2. MC simulation

The geometrical setup is shown in Fig. 2. First, the PDD and OAR at 10 cm depth were calculated without anything placed in water phantom, where these calculated data were compared with the measured data from the ionization chamber. The voxel size used for the calculation of the water absorbed dose was $5 \times 5 \times 5$ mm^3. For the simulation with the IP, the IP was placed perpendicular to the beam axis at a depth of 10 cm, and the OAR was obtained by calculating the dose to the phosphor layer. The voxel size used for this calculation was 5 mm $\times$ 5 mm $\times$ 210 μm. Figure 3 is a schematic showing the result of the calculation.

B. Investigating the filter by MC simulation

This calculation also followed the above procedure. The size of filters used in the simulation was 35×35 cm^2, and the filters were set, as shown in Fig. 4, in three different configurations: above only, below only, and one on each side simultaneously. The material, thickness, and displacement of the filters were varied. The same simulation was repeated without the IP and filters, from which the OAR was obtained and used as a reference for comparison. From the simulation, the appropriate filter was identified as the one for which the calculation result was closest to the OAR data without the IP. The following formula was used to determine which data gave the closest comparison,

$$(\text{relative error})_r(\%) = \frac{(\text{OAR}_{\text{IP},r} - \text{OAR}_{W,r})}{\text{OAR}_{W,0}} \times 100,$$

where $\text{OAR}_{\text{IP},r}$ is OAR on the IP (the phosphor layer) at r millimeters from the central axis. $\text{OAR}_{W,r}$ is OAR with the IP and the filter in r millimeters from the central axis and likewise $\text{OAR}_{W,0}$ is the one in 0 mm from central axis. Unless stated, the value for the OAR is computed with the arithmetic average of relative errors locating from -60 to -100 mm from central axis at a 10 cm depth, where the errors obviously show up, with a 10×10 cm^2 field size and 100 cm SSD.

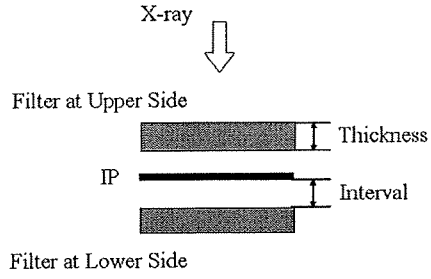

FIG. 4. Schematic diagram showing the location of double filters placed on both sides of the IP. The size of the filter was 35×35 cm^2. The material, thickness, and the distance between the IP and the filter were varied.

1. Material of the filters

The materials used in this evaluation are simple substances with atomic number (Z) from 4 to 82. Concerning the material data, the simulation was carried out in two ways, one simply using the density of every material,[22] the other setting the density to the one of lead, 11.35 g/cm^3, for all the materials in order to observe the Z dependency. The thickness was fixed to 2 mm and there was no gap between the filter and the IP.

2. Filter thickness

For this evaluation, only the lead filter was used. The filter thickness was varied from 0 to 15 mm and there was no gap between the filter and IP in the calculation.

3. Filters displacement

The lead filter was also used for this calculation. The distance between the IP and the filter (expressed by "Interval" in Fig. 4) was varied from 0 to 15 mm for two cases; filter thicknesses of 2 and 1 mm. We set water equivalent data in the interval.

III. RESULTS AND DISCUSSIONS

A. MC simulation parameter settings and evaluation

As reported by Olch,[11] the dependence of the pixel value from IP measurement on dose is given in Fig. 5, and this is expressed by a logarithmic relationship. The energy spectrum used in the simulation is shown in Fig. 6. For comparison, the results of the calculation and the measured PDD and OAR are shown in Fig. 7. As can be seen in Fig. 7(a), the calculated depth dose relationship is in good agreement with the measured data. From Fig. 7(b) we can find the average values of the relative error from -60 to -100 mm from the central axis with and without the IP. These are $20.7 \pm 2.6\%$ for the measurement and $20.5 \pm 3.0\%$ for the simulation, showing good agreement for the OAR. These results infer that the MC simulation settings used were realistic.

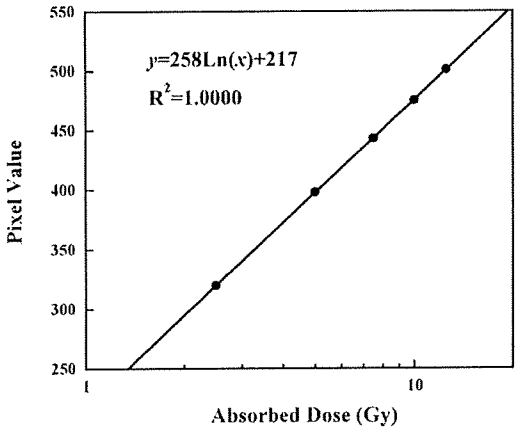

FIG. 5. Relationship between absorbed dose and pixel value along the central axis of a 10×10 cm^2 field in 10×10 mm^2.

B. Investigating the filter by MC simulation

The calculated OAR is shown in Fig. 8, which shows that, compared with the dose in water (dose with no IP in water), there is a $20.5\pm3.0\%$ difference in the average value of the relative error from -60 to -100 mm from central axis with the IP only, a $15.3\pm2.7\%$ difference for the IP with a 2 mm copper filter placed above it and a $9.8\pm2.2\%$ difference for the IP with a lead filter. It can be seen that the use of filters shifts the result closer to the dose in water with no IP.

First, we shall discuss the appropriate material to be used for the filter. A similar calculation to that shown in Fig. 8 was done for each material in order to determine the appropriate filter. The results are shown in Fig. 9. As the results show, placing a filter on each side of the IP produced a better effect than with a single filter on either side. In Fig. 9(a), compared to Ag($Z=47$) and Nd($Z=60$), Ba($Z=56$) has a higher relative error based on t-tests ($P<0.001$). This is because Ba has a density of 3.5 g/cm^3 and thus, compared with Ag (density: 10.5 g/cm^3) and Nd (density: 6.9 g/cm^3), has a smaller ratio between density and Z. On the other hand, Fig. 9(b) shows the Z dependency only for filter materials ($Z=4-82$), from which we can see that the effect produced by the filter improves as Z increases, and, as the results indicate, using a high density filter material on both sides leads to a much better effect. Considering the results and the materials that are practical to use, we conclude that Pb would be the most appropriate filter material.

Our second discussion is with regard to the filter thickness. The MC simulation results are shown in Fig. 10, which

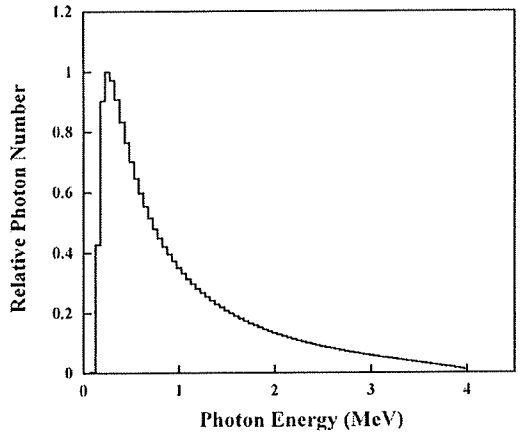

FIG. 6. Photon energy spectrum used in MC calculation.

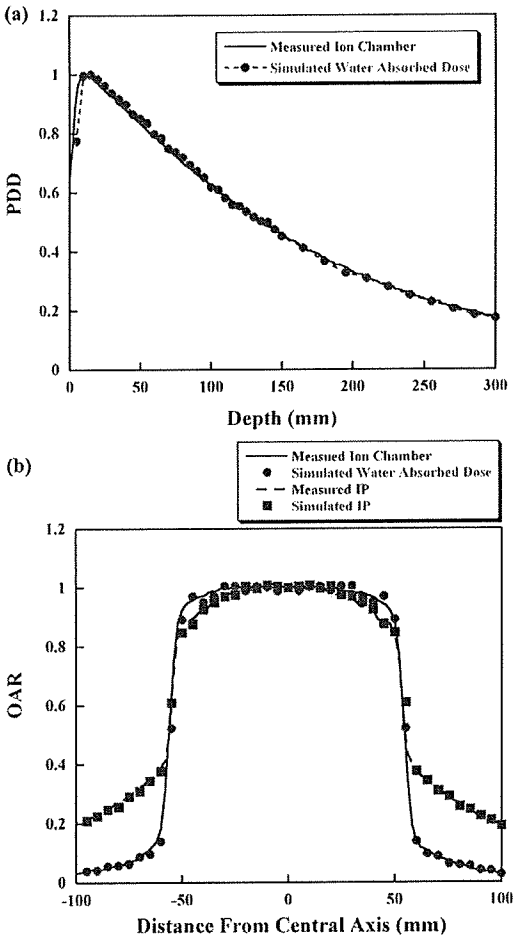

FIG. 7. Comparison of MC calculation with measurements. (a) PDD in beam axis. (b) OAR at 10 cm depth.

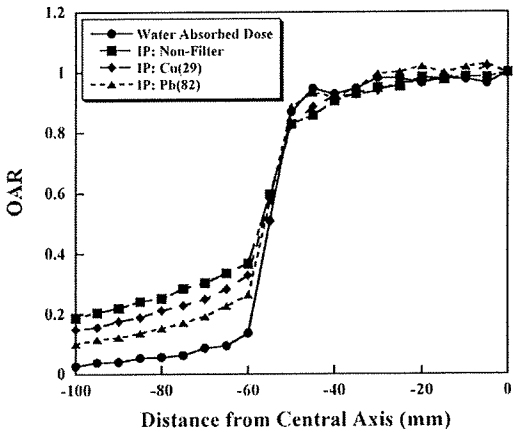

FIG. 8. Comparison of the OAR in water for nonfilter and 2 mm thick Cu and Pb filters where the filter is placed in contact with the IP.

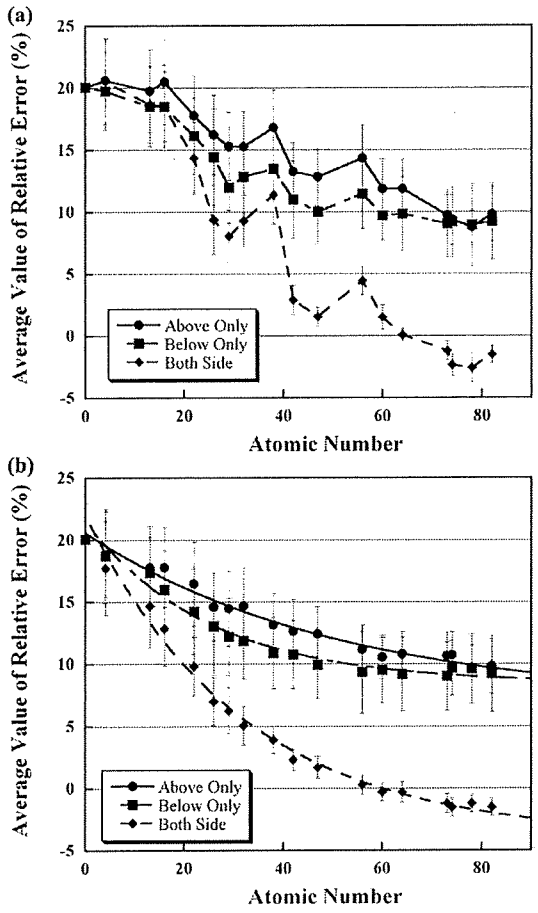

FIG. 9. Average value of relative error from −60 to −100 mm from the central axis for different filter materials. Atomic number 0 means that no filter is used. (a) Result using the density (g/cm^3) associated with each atomic number. (b) Similar to (a) but using a constant density value of 11.35 g/cm^3 for each atomic number material.

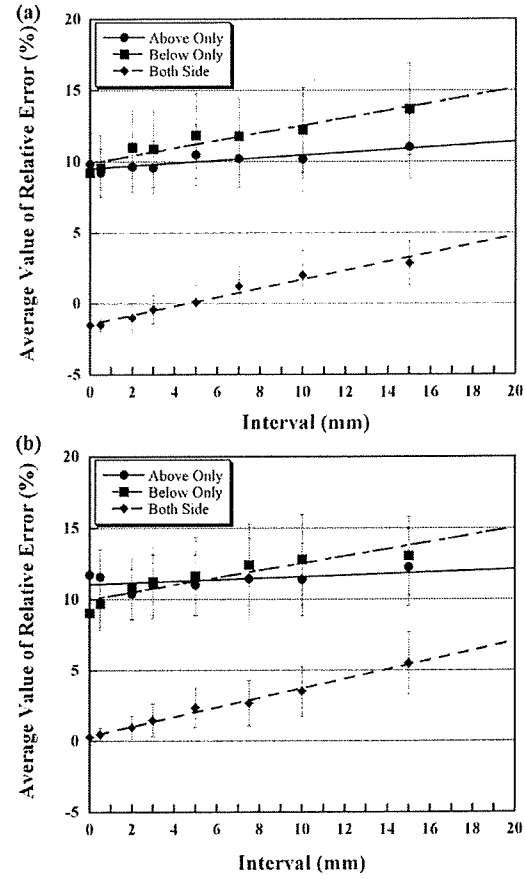

FIG. 11. Average value of relative error as a function of the distance between the filters and the IP (interval). Interval 0 means that these are in contact. (a) Average values of relative error using a 2 mm thick Pb filter. (b) Average values of relative error using a 1 mm thick Pb filter.

shows the relationship between the relative error and the thickness of the Pb filter from −60 to −100 mm from central axis. It can be seen that there is a general trend for the relative error to fall to a constant value as the filter thickness is increased. For the filter placed under the IP, this occurs for a thickness of 1 mm, and is due to the contribution of low

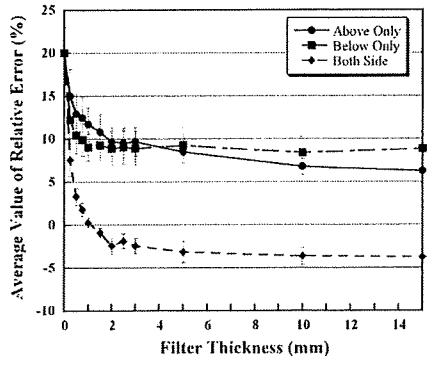

FIG. 10. Average value of relative error vs Pb filter thickness. Filter thickness 0 means no filter is used.

energy photons scattered from the IP. According to the results, good agreement was found between the calculated OAR without an IP and when using 1 mm thick Pb filters on each side of the IP. If filters thicker than 1 mm are used, the effect becomes excessive. As shown in Fig. 10, the gradient of the relative error curve is steep at 1 mm, so that, when making the filter, care should be taken in the precision of the thickness; for example, if the filter were to be 0.75 or 1.5 mm in thickness, relative errors of $1.8 \pm 0.8\%$ or $-0.9 \pm 0.6\%$, respectively, would arise.

So far we have determined the most suitable material and the thickness of the filter. Finally, we discuss the position of the filter with respect to the IP. The relationship between the relative error and the distance of the Pb filter from the IP was calculated. Figure 11 represents the results for 2 mm thick Pb filters [Fig. 11(a)] as well as 1 mm thick filters [Fig. 11(b)]. There is no significant position dependent effect observed for the filter placed above the IP; whereas, for ones placed beneath or on both sides of the IP, the relative errors increase linearly as the distance between the IP and the filter increases. It is indicated that the filter effect tends to diminish. The scattered photons basically have a lower energy spectrum and scatter into a larger solid angle. In addition to this, since the IP includes high atomic number (Z) materials,

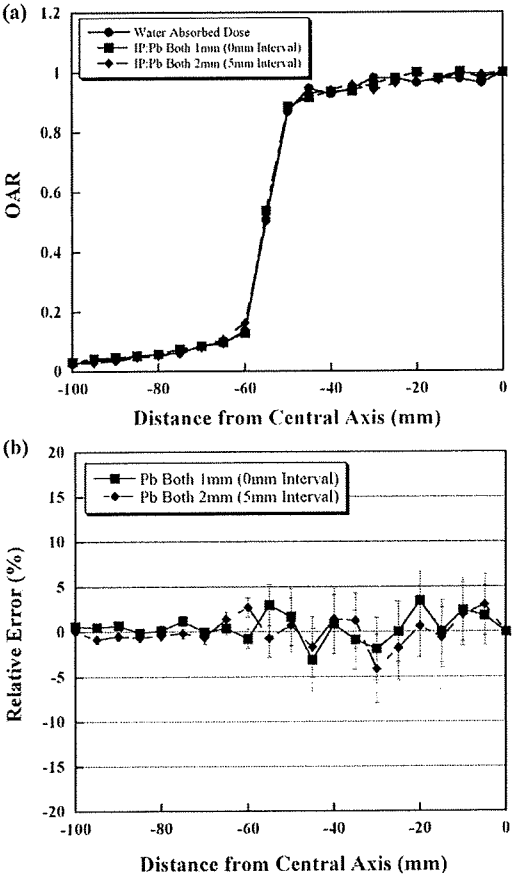

FIG. 12. (a) Comparison between the OAR calculated in water (no IP) and the OAR in water with an IP with 1 mm thick Pb filters and 2 mm thick Pb filters. (b) Relative error vs distance from the central axis.

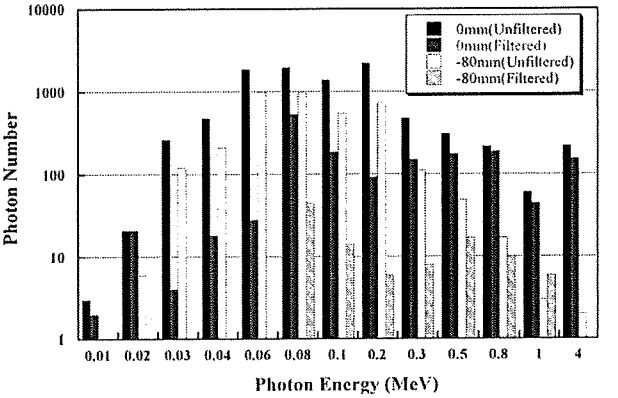

FIG. 13. Comparison of the energy spectra of photons (1×10^8 photons) interacting in the IP, on the beam axis and at −80 mm from the central axis for the cases with no filter and 1 mm thick Pb filters attached to each side of the IP.

such as Ba, the lower energy photons are attenuated much than higher ones. This is how the ratio of the energy given to IP by the backscattered photons from down stream of the IP is greater than that by photons scattered from upper stream of IP where water exist between the IP and the filter and the scatter is caused mainly by interaction with water. Therefore, the contribution to the IP of photons backscattered from under the IP is much larger than photons scattered from the upper side of the IP. This is the reason, if the interval is large, the filter position affects the relative errors. Essentially, the best options for position found from the results are with filters placed on each side of the IP, either with 2 mm Pb filters with a 5 mm interval or 1 mm Pb filters with a 0 mm interval (i.e., filters attached to both sides of the IP). Note that precision is also needed when placing the filters at the recommended distances. The OARs of the optimum filter positions and that without an IP (OAR in water) are shown in Fig. 12(a). In addition, the relative errors derived from the results in Fig. 12(a) are shown in Fig. 12(b), which showed that the relative errors of 1 mm Pb filters with a 0 mm interval and 2 mm Pb filters with a 5 mm interval distributed around 0% both in and out of the field. There was a good agreement with the result of the water absorbed dose. In detail, we calculated the root mean square of the relative error in terms of out-of-field (from −60 to −100 mm) and in-field (from 0 to −50 mm). The results of 1 and 2 mm thick Pb filters were 2.0% and 2.0% in the field and 0.6% and 1.1% out of the field, respectively. Thus, this simulation study indicated that, by using two 1 mm thick Pb filters attached to each side of the IP or two 2 mm thick Pb filters placed 5 mm from each side of the IP, it is possible to obtain OAR curve with IP as accurate as the one based on the absorbed dose calculated only in water.

We also investigated the energy spectra in the IP with and without filters. We calculated the energy spectrum in each case from the MC analysis and the results are shown in Fig. 13. What the figure shows is that the number of photons in the low energy range (especially keV range), where there is an energy dependency on the IP, is reduced by the filter. Thus, the accuracy of the IP measurement is improved when the filter is used. The OAR measurement, in particular, can be done without concern about the energy dependency of the IP.

In study of Olch,[11] a 0.4 mm Pb filter was placed on both sides of an IP and a 6 MV photon OAR measurement was done. This is different from our study where 1 mm Pb filters were attached to both sides of the IP. What we have done in our study is completely different to his research with respect to using different IPs, energies, different procedures, and so on. To make a comparison with his study and also to develop a more reliable filter, a further more detailed study using more sophisticated calculation conditions would be needed. Additionally a certain distance of 5 mm from each side of the IP obtained in this study was suggested as one of parameters for using the Pb filters as simply as possible. This was the result that we tried to figure out some parameters as less as possible, by which it is expected that the quality assurance would be performed easily and quickly. However, it may also be important that the consideration of specific parameters suitable for each measurement condition would be needed to investigate the possibility of use of IP as a quality assurance tool with high accuracy.

[1] L. Stanton, Radiology **78**, 445 (1962).
[2] J. F. Williamson, F. M. Khan, and S. C. Sharma, Med. Phys. **8**, 94 (1981).
[3] C. W. Cheng and I. J. Das, Med. Phys. **23**, 1225 (1996).

[4] P. Cadman, Med. Phys. **25**, 1435 (1998).
[5] M. D. R. Thomas and A. P. Warrington, Phys. Med. Biol. **51**, 1439 (2006).
[6] M. Fuss, E. Sturtewagen, C. D. Wagter, and D. Georg, Phys. Med. Biol. **52**, 4211 (2007).
[7] L. J. van Battum, D. Hoffmans, H. Piersma, and S. Heukelom, Med. Phys. **35**, 704 (2008).
[8] M. Sonoda, M. Takano, J. Miyahara, and H. Kato, Radiology **148**, 833 (1983).
[9] J. A. Rowlands, Phys. Med. Biol. **47**, R123 (2002).
[10] S. M. Kengyelics, A. G. Davies, and A. R. Cowen, Med. Phys. **25**, 2163 (1998).
[11] A. J. Olch, Med. Phys. **32**, 2987 (2005).
[12] M. Homma, K. Tabushi, Y. Obata, T. Tamiya, S. Koyama, and T. Ishigaki, Jpn. J. Med. Phys. **22**, 118 (2002).
[13] H. H. Li, A. L. Gonzalez, H. Ji, and M. Duggan, Med. Phys. **34**, 103 (2007).
[14] S. E. Burch, K. J. Kearfott, J. H. Trueblood, W. C. Shiels, J. I. Yeo, and C. K. Wang, Med. Phys. **24**, 775 (1997).
[15] I. J. Yeo, C. K. Wang, and S. E. Burch, Med. Phys. **24**, 1943 (1997).
[16] S. G. Ju, Y. C. Ahn, S. J. Huh, and I. J. Yeo, Med. Phys. **29**, 351 (2002).
[17] S. Agostinelli, J. Allison, K. Amako, J. Apostolakis, H. Araujo, P. Arce, M. Asai, D. Axen, S. Banerjee, G. Barrabd, F. Behner, *et al.*, Nucl. Instrum. Methods Phys. Res. A **506**, 250 (2003).
[18] L. I. Schiff, Phys. Rev. **83**, 252 (1951).
[19] G. E. Desobry and A. L. Boyer, Med. Phys. **18**, 497 (1991).
[20] C. R. Baker, B. Ama'ee, and N. M. Spyrou, Phys. Med. Biol. **40**, 529 (1995).
[21] M. Partridge, Phys. Med. Biol. **45**, N115 (2000).
[22] S. M. Seltzer and J. H. Hubblell, *Photon Attenuation Coefficient Data Book* (Japan Society of Radiological Technology, Kyoto, 1995).